Supplementary Information for

Nanomechanical footprint of SARS-CoV-2 variants in complex with a potent nanobody by molecular simulations

Luis F. Cofas-Vargas[*1], Gustavo E. Olivos-Ramirez[1], Mateusz Chwastyk[2], Rodrigo A. Moreira[3], Joseph L. Baker[4], Siewert J. Marrink[5], Adolfo B. Poma*[*1]*

[1]Biosystems and Soft Matter Division, Institute of Fundamental Technological Research, Polish Academy of Sciences, ul. Pawińskiego 5B, 02-106 Warsaw, Poland
[2]Institute of Physics, Polish Academy of Sciences, al. Lotników 32/46, 02-668 Warsaw, Poland
[3]Basque Center for Applied Mathematics, Mazarredo 14, 48009 Bilbao, Spain
[4]Department of Chemistry, The College of New Jersey, 2000 Pennington Road, Ewing, NJ 08628, USA
[5]Groningen Biomolecular Sciences and Biotechnology Institute, University of Groningen, Nijenborgh 7, 9747 AG Groningen, The Netherlands.

This file includes:

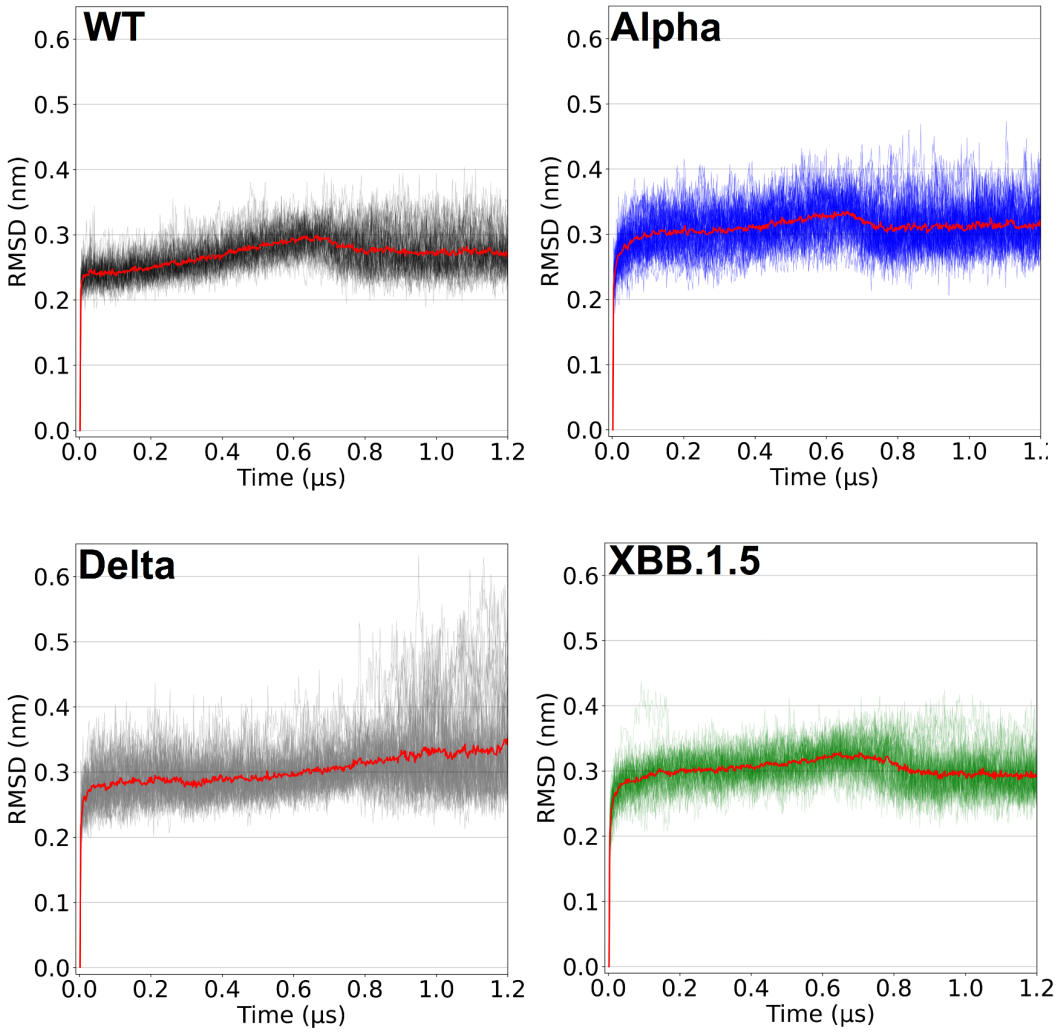

Figure S1. RMSD analysis of RBD variants. The figure depicts the RMSD values for each variant, with the red line representing the average RMSD. These values indicate that minimal conformational changes occurred during the pulling event.

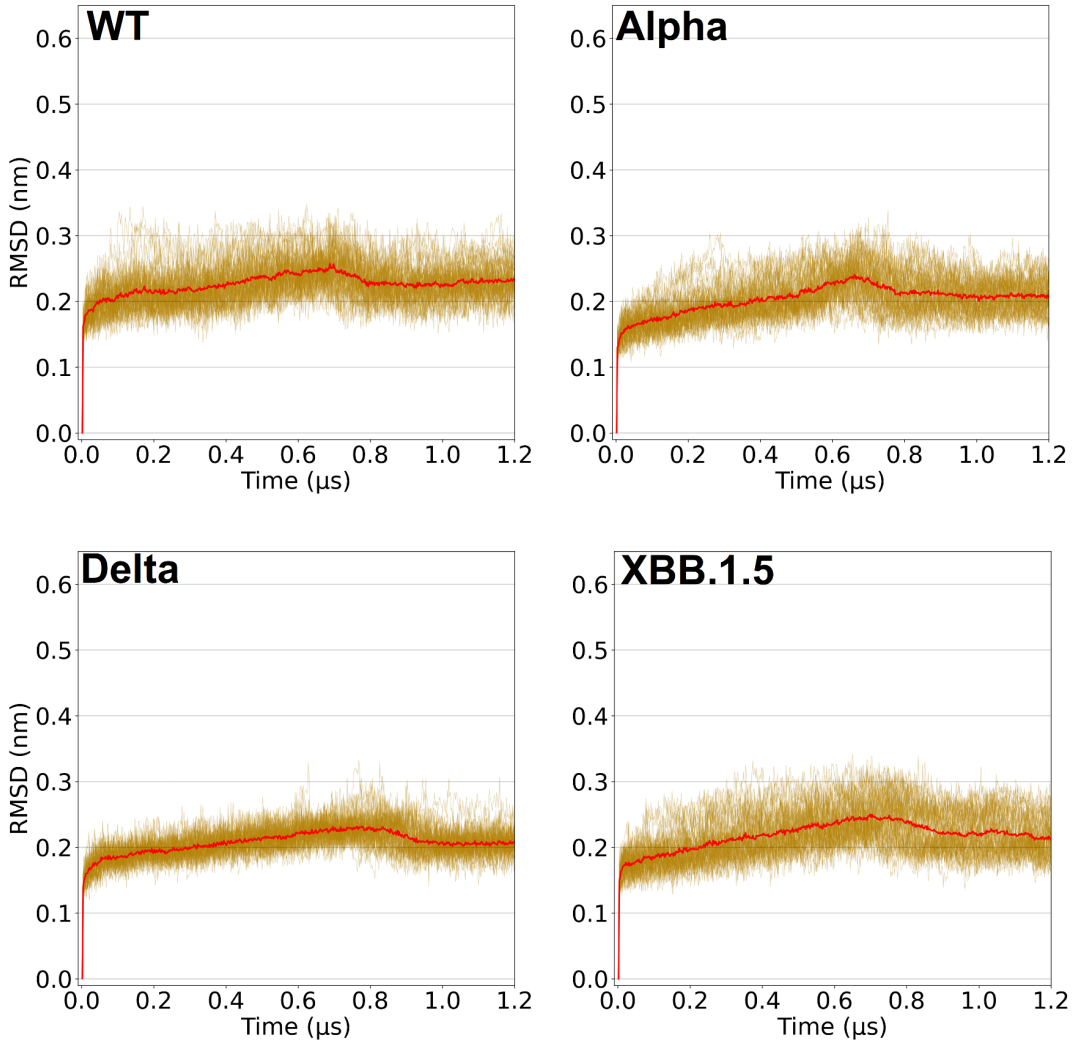

Figure S2. RMSD analysis for the H11-H4 nanobody for each complex. The red line indicates the average RMSD. Minimal conformational changes observed during the pulling event suggest that the nanobody is stable under mechanical stress.

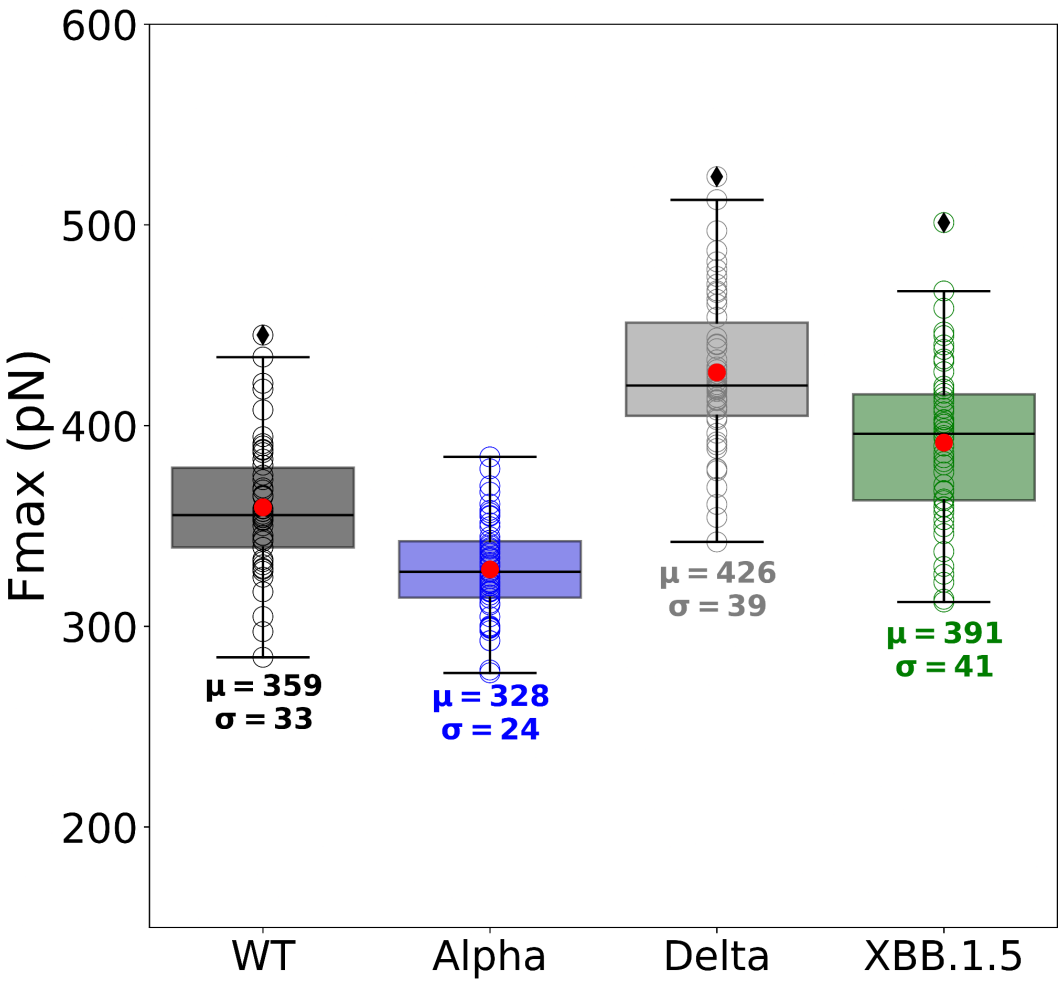

Figure S3. Distribution of forces required for the mechanical dissociation of the RBD-H11-H4 complexes. The external forces (pN) applied to various RBD variants are shown as a box plot. The median force is represented by the horizontal line within each box, while the average force is represented by a red circle.

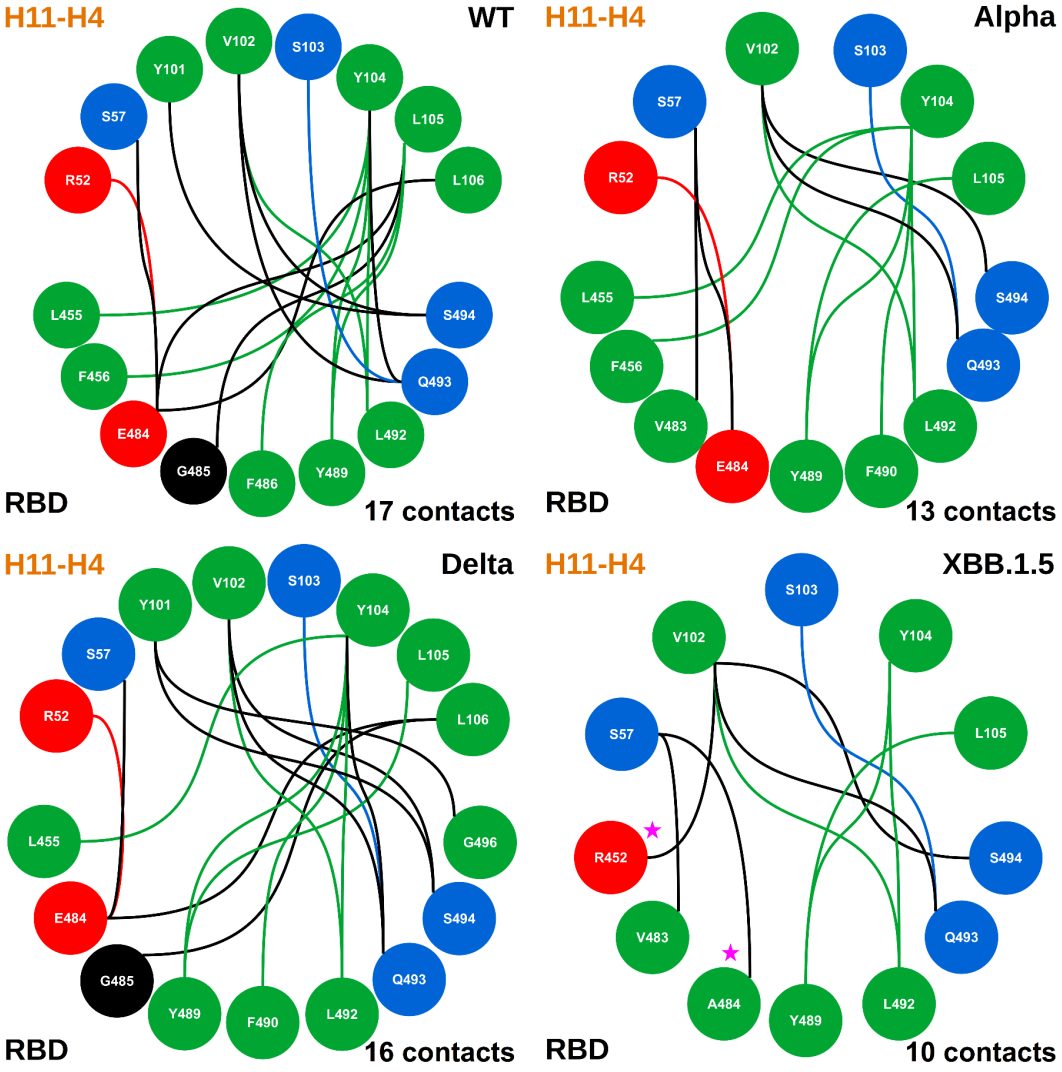

Figure S4. Network representation of native contacts within the RBD-H11-H4 interface at Fmax. The lines represent the pairs of contacts. The color of the lines represents the type of interaction: red for ionic, blue for polar, green for nonpolar, and black for non-specific interactions. The amino acid residues are colored based on their chemical properties. Stars in magenta indicate mutations.

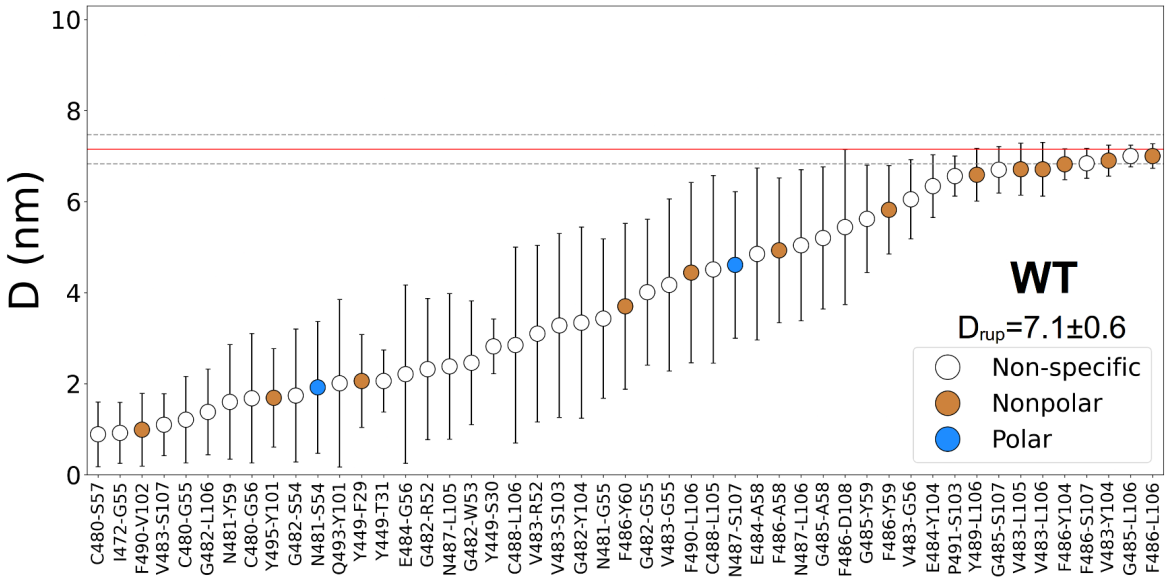

Figure S5. Dissociation profiles of non-native contacts (NON) in the RBD_{WT}-H11-H4 complex. The contact pairs are located on the X-axis, whereas the Y-axis denotes the displacement (D) of the virtual site particle in the Z-direction, as measured in nanometers (nm). The average lengths of dissociation are depicted, with error bars indicating the standard deviation. Contacts are color-coded: white for non-specific, brown for nonpolar, and blue for polar interactions.

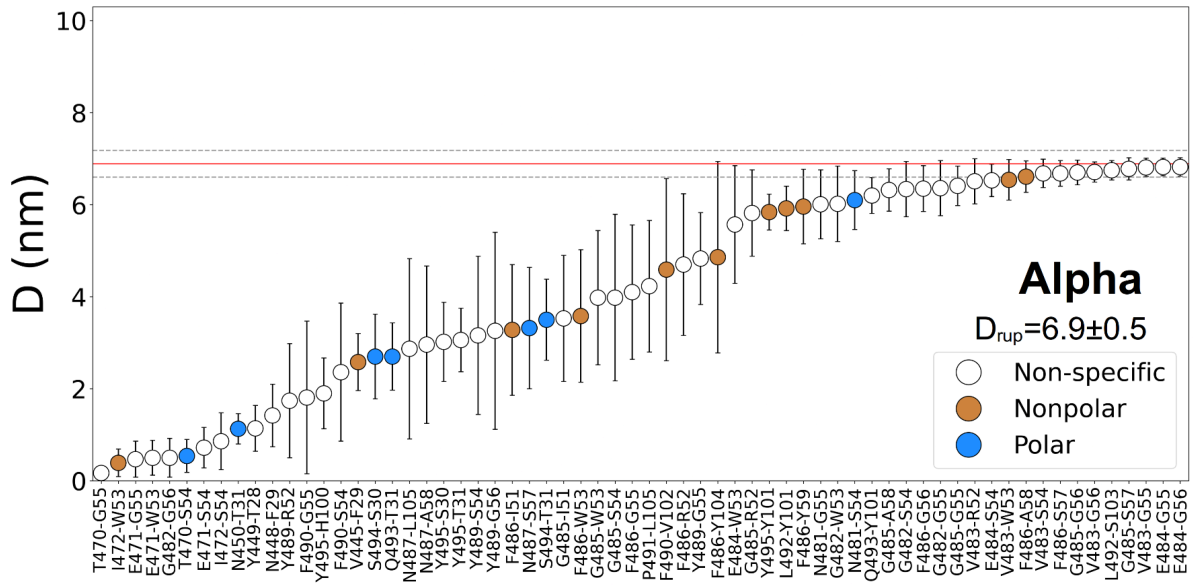

Figure S6. Dissociation profiles of non-native contacts (NON) in the RBD_{Alpha}-H11-H4 complex. The contact pairs are located on the X-axis, whereas the Y-axis denotes the displacement (D) of the virtual site particle in the Z-direction, as measured in nanometers (nm). The average lengths of dissociation are depicted, with error bars indicating the standard deviation. Contacts are color-coded: white for non-specific, brown for nonpolar, and blue for polar interactions.

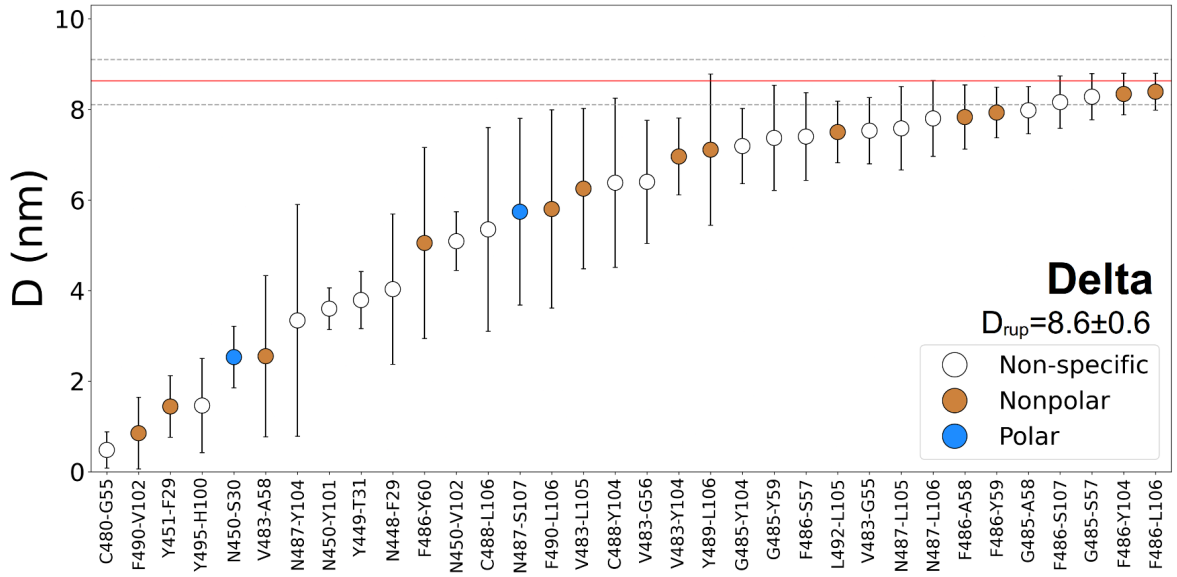

Figure S7. Dissociation profiles of non-native contacts (NON) in the RBD_{Delta}-H11-H4 complex. The contact pairs are located on the X-axis, whereas the Y-axis denotes the displacement (D) of the virtual site particle in the Z-direction, as measured in nanometers (nm). The average lengths of dissociation are depicted, with error bars indicating the standard deviation. Contacts are color-coded: white for non-specific, brown for nonpolar, and blue for polar interactions.

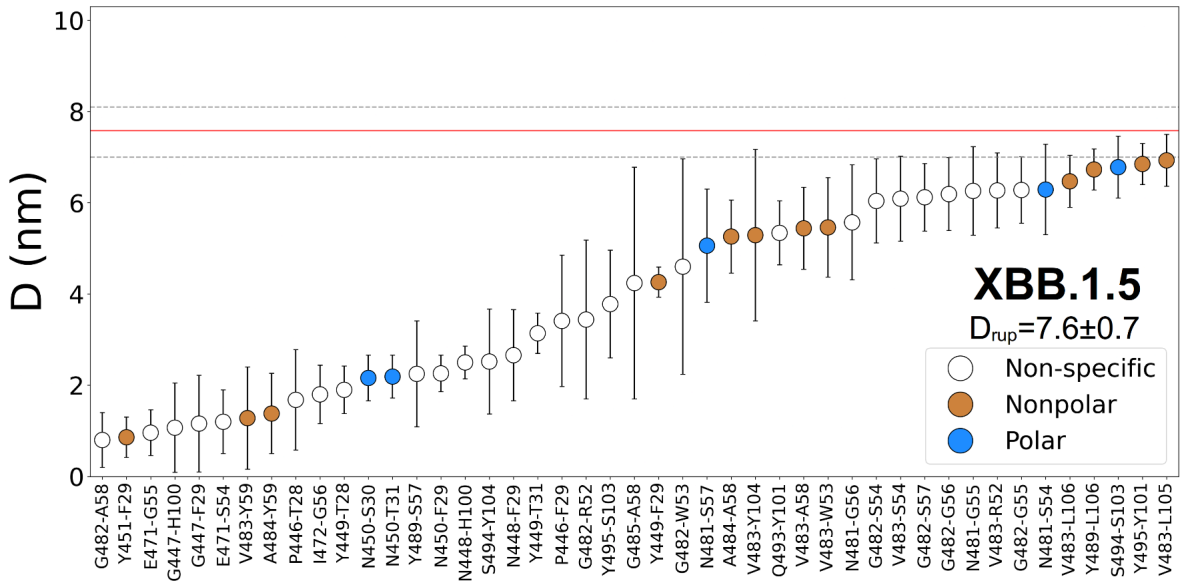

Figure S8. Dissociation profiles of non-native contacts (NON) in the $RBD_{XBB.1.5}$-H11-H4 complex. The contact pairs are located on the X-axis, whereas the Y-axis denotes the displacement (D) of the virtual site particle in the Z-direction, as measured in nanometers (nm). The average lengths of dissociation are depicted, with error bars indicating the standard deviation. Contacts are color-coded: white for non-specific, brown for nonpolar, and blue for polar interactions.

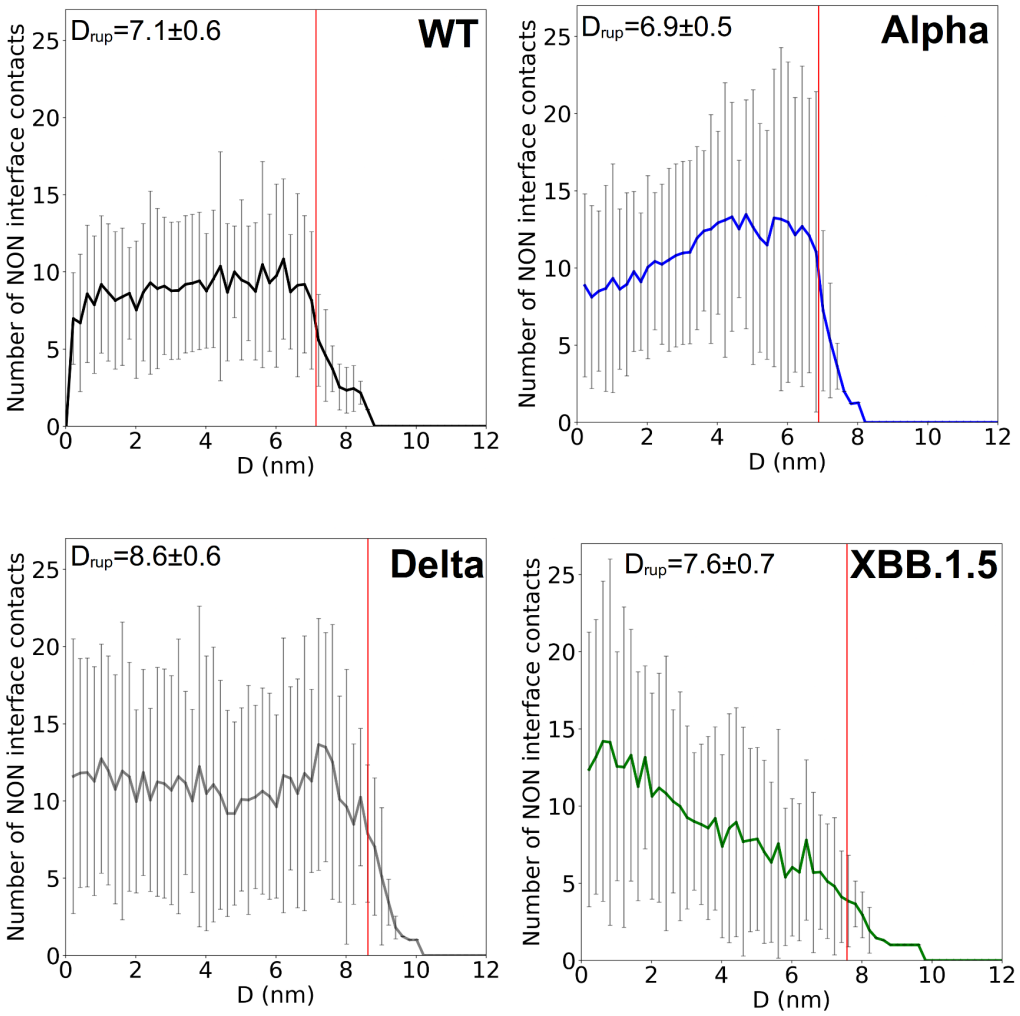

Figure S9. Profile of non-native interface contacts observed during GōMartini pulling simulations of RBD-H11-H4 complexes. NON contacts were analyzed across a collection of 50 pulling trajectories. The red vertical line indicates the average rupture distance of the complex. The gray lines depict the standard deviation.

Table S1. Two-Tailed P-Values Comparing SARS-CoV-2 Variants (WT, Alpha, Delta, XBB.1.5). Statistical analysis was conducted to assess the significance of differences between variants based on mean and average measurements (n=50).

Variant	WT	Alpha	Delta	XBB.1.5
WT	-	1.279×10^{-06}	3.100×10^{-12}	5.591×10^{-05}
Alpha	1.279×10^{-06}	-	5.639×10^{-17}	3.419×10^{-12}
Delta	3.100×10^{-12}	5.639×10^{-17}	-	
XBB.1.5	5.591×10^{-05}	3.419×10^{-12}	5.119×10^{-05}	-

Table S2. List of protein contacts at RBD/H11-H4 interface. Protein-protein interactions are calculated using the OV+rCSU contact map protocol over an MD trajectory of 1 μs. Protein contacts with a frequency of 0.7 were considered in the contact map. The total number of protein contacts is given next to the RBD variant name.

WT (24)	Alpha (21)	Delta (22)	XBB.1.5 (16)
N450-H100	N450-H100	N450-H100	-
Y449-D115	-	Y449-D115	-
Y449-Y101	Y449-Y101	Y449-Y101	Y449-Y101
F490-Y104	F490-Y104	F490-Y104	S490-Y104
L452-V102	L452-V102	L452-V102	R452-V102
F490-R52	F490-R52	F490-R52	S490-R52
Y449-H100	Y449-H100	Y449-H100	Y449-H100
E484-R52	E484-R52	E484-R52	A484-R52
Y489-Y104	Y489-Y104	Y489-Y104	Y489-Y104
Q493-V102	Q493-V102	Q493-V102	Q493-V102
S494-V102	S494-V102	S494-V102	S494-V102
L492-V102	L492-V102	L492-V102	L492-V102
S494-Y101	S494-Y101	S494-Y101	-
L455-Y104	L455-Y104	L455-Y104	-
L492-Y104	L492-Y104	L492-Y104	L492-Y104
Q493-S103	Q493-S103	Q493-S103	Q493-S103
Q493-Y104	Q493-Y104	Q493-Y104	-
F456-Y104	F456-Y104	-	F456-Y104
E484-L105	-	-	-
F486-L105	-	-	-
E484-S57	E484-S57	E484-S57	-
E484-L106	E484-L106	E484-L106	-
G485-L105	-	-	-
Y489-L105	Y489-L105	Y489-L105	Y489-L105
-	V483-S57	-	V483-S57
-	-	G485-L106	-
-	-	G496-Y101	-

-	-	-	A484-S57

Table S3. List of non-native interactions during the pulling simulations. Protein contacts were calculated using the definition of enlarged VdW radii as reported by [1]. Total number of protein contacts is given next to the RBD variant name.

WT (49)	Alpha (64)	Delta (34)	XBB.1.5 (45)
C480-S57	-	-	-
I472-G55	-	-	-
F490-V102	F490-V102	F490-V102	-
V483-S107	-	-	-
C480-G55	-	C480-G55	-
G482-L106	-	-	-
N481-Y59	-	-	-
C480-G56	-	-	-
Y495-Y101	Y495-Y101	-	Y495-Y101
G482-S54	G482-S54	-	G482-S54
N481-S54	N481-S54	-	N481-S54
Q493-Y101	Q493-Y101	-	Q493-Y101
Y449-F29	-	-	Y449-F29
Y449-T31	-	Y449-T31	Y449-T31
E484-G56	E484-G56	-	-
G482-R52	-	-	G482-R52
N487-L105	N487-L105	N487-L105	-
G482-W53	G482-W53	-	G482-W53
Y449-S30	-	-	-
C488-L106	-	C488-L106	-
V483-R52	V483-R52	-	V483-R52
V483-S103	-	-	-
G482-Y104	-	-	-
N481-G55	N481-G55	-	N481-G55
F486-Y60	-	F486-Y60	-
G482-G55	G482-G55	-	G482-G55
V483-G55	V483-G55	V483-G55	-
F490-L106	-	F490-L106	-

C488-L105	-	-	-
N487-S107	-	N487-S107	-
E484-A58	-	-	A484-A58
F486-A58	F486-A58	F486-A58	-
N487-L106	-	N487-L106	-
G485-A58	G485-A58	G485-A58	G485-A58
F486-D108	-	-	-
G485-Y59	-	G485-Y59	-
F486-Y59	F486-Y59	F486-Y59	-
V483-G56	V483-G56	V483-G56	-
E484-Y104	-	-	-
P491-S103	-	-	-
Y489-L106	-	Y489-L106	Y489-L106
G485-S107	-	-	-
V483-L105	-	V483-L105	V483-L105
V483-L106	-	-	V483-L106
F486-Y104	F486-Y104	F486-Y104	-
F486-S107	-	F486-S107	-
V483-Y104	-	V483-Y104	V483-Y104
G485-L106	-	-	-
F486-L106	-	F486-L106	-
-	T470-G55	-	-
-	I472-W53	-	-
-	E471-G55	-	E471-G55
-	E471-W53	-	-
-	G482-G56	-	G482-G56
-	T470-S54	-	-
-	E471-S54	-	E471-S54
-	I472-S54	-	-
-	N450-T31	-	N450-T31
-	Y449-T28	-	Y449-T28
-	N448-F29	N448-F29	N448-F29

-	Y489-R52	-	-
-	F490-G55	-	-
-	Y495-H100	Y495-H100	-
-	F490-S54	-	-
-	V445-F29	-	-
-	S494-S30	-	-
-	Q493-T31	-	-
-	N487-A58	-	-
-	Y495-S30	-	-
-	Y495-T31	-	-
-	Y489-S54	-	-
-	Y489-G56	-	-
-	F486-I51	-	-
-	N487-S57	-	-
-	S494-T31	-	-
-	G485-I51	-	-
-	F486-W53	-	-
-	G485-W53	-	-
-	G485-S54	-	-
-	F486-G55	-	-
-	P491-L105	-	-
-	F486-R52	-	-
-	Y489-G55	-	-
-	E484-W53	-	-
-	G485-R52	-	-
-	L492-Y101	-	-
-	F486-G56	-	-
-	G485-G55	-	-
-	E484-S54	-	-
-	V483-W53	-	V483-W53
-	V483-S54	-	V483-S54
-	F486-S57	F486-S57	-

-	G485-G56	-	-
-	L492-S103	-	-
-	G485-S57	G485-S57	-
-	E484-G55	-	-
-	-	Y451-F29	Y451-F29
-	-	N450-S30	N450-S30
-	-	V483-A58	V483-A58
-	-	N487-Y104	-
-	-	N450-Y101	-
-	-	N450-V102	-
-	-	C488-Y104	-
-	-	G485-Y104	-
-	-	L492-L105	-
-	-	-	G482-A58
-	-	-	G447-H100
-	-	-	G447-F29
-	-	-	V483-Y59
-	-	-	A484-Y59
-	-	-	P446-T28
-	-	-	P446-F29
-	-	-	I472-G56
-	-	-	N450-F29
-	-	-	Y489-S57
-	-	-	N448-H100
-	-	-	S494-Y104
-	-	-	S494-S103
-	-	-	G482-S57
-	-	-	Y495-S103
-	-	-	N481-S57
-	-	-	N481-G56

Table S4. The interface energy of RBD/H11-H4 for SARS-CoV-2 variants in Martini 3 simulations. Interface energies for different variants using the Martini 3 force and GōMartini 3 approach. The coarse-grained topologies were created as described in the Methods sections, using a cubic box extending 2 nm beyond the solute in each direction. A 1 μs long trajectory was run for each variant. For each trajectory, the Van der Waals and electrostatics contribution were calculated for the complex, and for each individual protein using the energy module of GROMACS. The respective contribution of each protein was subtracted from the complex to obtain the interface energy given by the Martini 3 force field. Additionally, the energetic contribution for each Gō contact at the was calculated for each frame, and the total interaction per frame was averaged over each trajectory.

	Martini 3 force field			
Variant	**Van der Waals (kJ/mol)**	**Electrostatics (kJ/mol)**	**Gō potentials (kJ/mol)**	**Total interface energy (kJ/mol)**
WT	-366.8±36.1	-4.5±2.6	-286.5±12.3	-657.7±38.2
Alpha	-421.0±61.5	-4.3±1.5	-226.5±14.6	-651.8±63.2
Delta	-401.0±33.5	-1.2±1.8	-280.4±9.3	-682.7±34.9
XBB.1.5	-349.5±28.1	-3.2±5.0	-197.8±10.3	-550.5±30.3

References

1 M. Chwastyk, A. P. Bernaola and M. Cieplak, *Phys. Biol.*, 2015, **12**, 046002.